Title

Electrostatic carrier doping of GdTiO3/SrTiO3 interfaces

Journal

Applied Physics Letters, 99(23)

Authors

Moetakef, Pouya
Cain, Tyler
Ouellette, Daniel
et al.

Publication Date

2011-12-09

Peer reviewed

Electrostatic carrier doping of $GdTiO_3/SrTiO_3$ interfaces

Pouya Moetakef,[1] Tyler A. Cain,[1] Daniel G. Ouellette,[2] Jack Y. Zhang,[1] Dmitri O. Klenov,[3] Anderson Janotti,[1] Chris G. Van de Walle,[1] Siddharth Rajan,[4] S. James Allen,[2] and Susanne Stemmer[1,a)]

[1]*Materials Department, University of California, Santa Barbara, California, 93106-5050, USA*
[2]*Department of Physics, University of California, Santa Barbara, California, 93106-9530, USA*
[3]*FEI, Achtseweg Noord 5, 5651 GG Eindhoven, The Netherlands*
[4]*Department of Electrical and Computer Engineering, The Ohio State University, Columbus, Ohio 43210, USA*

(Received 28 October 2011; accepted 17 November 2011; published online 9 December 2011)

Heterostructures and superlattices consisting of a prototype Mott insulator, $GdTiO_3$, and the band insulator $SrTiO_3$ are grown by molecular beam epitaxy and show intrinsic electronic reconstruction, approximately $^1/_2$ electron per surface unit cell at each $GdTiO_3/SrTiO_3$ interface. The sheet carrier densities in all structures containing more than one unit cell of $SrTiO_3$ are independent of layer thicknesses and growth sequences, indicating that the mobile carriers are in a high concentration, two-dimensional electron gas bound to the interface. These carrier densities closely meet the electrostatic requirements for compensating the fixed charge at these polar interfaces. Based on the experimental results, insights into interfacial band alignments, charge distribution, and the influence of different electrostatic boundary conditions are obtained. © *2011 American Institute of Physics*. [doi:10.1063/1.3669402]

Two-dimensional electron gases (2DEGs) at interfaces between Mott insulators and band insulators have attracted significant attention because of unique properties, such as strong electron correlations, superconductivity, or magnetism.[1–7] Furthermore, interfaces between the band insulator $SrTiO_3$ and the rare earth titanates ($RTiO_3$, where R is a trivalent rare earth ion), which are Mott insulators, exhibit a fixed polar charge. In particular, $R^{3+}O^{2-}$ and $Ti^{3+}O_2^{4-}$ layers alternate along the (001) surface normal of $RTiO_3$,[8] carrying formal $+1$ and -1 charges, respectively, which causes a diverging electrostatic surface energy due to the non-zero dipole moment on the RO-TiO_2 units. At the interface, these transition to a sequence of neutral layers, $Sr^{2+}O^{2-}$ and $Ti^{4+}O_2^{4-}$, of non-polar (001) $SrTiO_3$. The fixed interfacial charge can be compensated by a 2DEG, residing in the bands of the Mott and/or band insulator and bound to the interface by the fixed charge.[9,10] In the absence of any other charge compensation, defects, interfacial mixing, roughness, and nonstoichiometry,[11–13] the interface is expected to form an extremely high-density 2DEG on the order of $3 \times 10^{14}\,cm^{-2}$, as given by $e/2S$, where S is the surface unit cell area and e the elementary charge. The nature and spatial distribution of charge carriers are of paramount importance for the properties of these heterostructures.

To date, attention has focused on $LaAlO_3/SrTiO_3$ and $LaTiO_3/SrTiO_3$ interfaces grown by pulsed laser deposition.[1,14–16] Results from electrical transport measurements vary significantly; in particular, $LaAlO_3/SrTiO_3$ interfaces show carrier densities that are an order of magnitude less than predicted from intrinsic electronic reconstruction.[17–19] Compensating mobile electrons are easily accessible for $RTiO_3/SrTiO_3$ structures as can be visualized by considering the atomically sharp interface as a 50:50 mixture of $RTiO_3$ and $SrTiO_3$, which has the required free electron density.[20] Transport and optical measurements of $LaTiO_3/SrTiO_3$ interfaces reveal densities close to those expected for electronic reconstruction,[16,21] but interpretation is complicated by conduction by non-interfacial carriers from both substrates and films[15,16]; $LaTiO_3$ films reported in the literature are often metallic.[22] This letter reports on transport measurements of the 2DEGs at $GdTiO_3/SrTiO_3$ interfaces (electronically analogous to $LaTiO_3/SrTiO_3$ (Refs. 23 and 24)) grown by molecular beam epitaxy (MBE) that exhibit an interfacial density with values that are essentially those predicted by electronic reconstruction. Theoretical band offsets between the conduction bands of $SrTiO_3$ and $GdTiO_3$ are used to model the spatial extent of the 2DEG.

The vastly different oxygen pressures required to obtain insulating $SrTiO_3$ and $GdTiO_3$ layers present an experimental challenge: high oxygen pressure is needed for insulating $SrTiO_3$ while $GdTiO_3$ films need to be grown under low oxygen pressure conditions to avoid metallic conductivity or formation of pyrochlore.[25,26] We use (001) surfaces of $(LaAlO_3)_{0.3}(Sr_2AlTaO_6)_{0.7}$ (LSAT) as substrates to avoid substrate conduction. All layers and superlattices were grown by MBE. $SrTiO_3$ was grown by co-deposition[27] whereas $GdTiO_3$ was grown by shuttered growth, supplying alternating monolayer doses of Gd and Ti tetra isopropoxide (TTIP), which supplied both Ti and oxygen. No additional oxygen was supplied.[28] For $GdTiO_3$ on $SrTiO_3$, growths were started and terminated with a TiO_2 layer. All layers and superlattices were coherently strained to the LSAT.[29] Aberration-corrected scanning transmission electron microscopy (FEI Titan G2 ChemiSTEM) was used to characterize the atomic structure of $GdTiO_3/SrTiO_3$ interfaces. Longitudinal and Hall resistivity were measured in Van der Pauw geometry using a Physical Properties Measurement System (Quantum Design PPMS). Ohmic contacts were 300 nm Au/20 nm Ni/40 nm Al for

a)Electronic mail: stemmer@mrl.ucsb.edu.

$SrTiO_3$ top layers and 300 nm Au/50 nm Ti for $GdTiO_3$ top layers. The top layer was Au for wire bonding with an Au wire.

The sheet resistances of $GdTiO_3$ grown directly on LSAT and of $GdTiO_3$ grown on $SrTiO_3$ buffer layers with different thicknesses are shown in Fig. 1(a). The $GdTiO_3$ film on LSAT with no $SrTiO_3$ buffer layer is insulating. While too resistive for meaningful Hall measurements, the Seebeck coefficient was measured and is positive (p-type), as found for stoichiometric $GdTiO_3$.[23] All bilayers are *n*-type and metallic if the $SrTiO_3$ thickness exceeded one unit cell (0.4 nm). Even the bilayer with one unit cell $SrTiO_3$ already exhibits a remarkable drop in resistance. The localized behavior for this sample is expected as the sheet resistance exceeds the critical Mott value ($\sim$10 k$\Omega/\square$). The sheet resistance should decrease with increasing $SrTiO_3$ thickness if the conductivity is due to the oxygen deficient $SrTiO_3$. The constant sheet resistance for $SrTiO_3$ layers thicker than 20 nm indicates that it arises from a space charge layer of constant thickness and carrier density at the interface. The Hall resistance as a function of magnetic field B was linear and *n*-type down to the lowest temperatures,[29] in contrast to $LaTiO_3/SrTiO_3$ (Refs. 15 and 16). All of the electrons contributing to the Hall resistance satisfy $\mu B \ll 1$. Although more than one subband with different mobility may be occupied, the Hall coefficient (R_H) is converted to an effective sheet density by $n_S = 1/eR_H$, where e is the elementary charge. Figure 1(b) shows that n_S is constant, $\sim 3.5 \times 10^{14}\,\mathrm{cm}^{-2}$, for all bilayers, even for extremely thin $SrTiO_3$. Thus there is little trapping at the LSAT/$SrTiO_3$ interface, at least on a scale of $\sim 3 \times 10^{14}\,\mathrm{cm}^{-2}$. A similar result is obtained when the $GdTiO_3$ thickness is varied. The mobility increases with $SrTiO_3$ thickness [Fig. 1(b)]. Thus the decrease in sheet resistance for $SrTiO_3$ layers between 0.4 nm and 20 nm is due to an increase in mobility, not a change in sheet carrier concentration. The results are consistent with an interfacial mobile space charge layer of constant thickness with a sheet charge density of $\sim 3 \times 10^{14}\,\mathrm{cm}^{-2}$. This carrier density closely corresponds to the $\frac{1}{2}$ electron per surface unit cell required to compensate for the polar discontinuity at the interface.

To further confirm the results, multilayer samples were investigated. Figure 2(a) shows the sheet carrier density for $(SrTiO_3/GdTiO_3/SrTiO_3)_x$ superlattices on LSAT as a function of the number of repeats x, each containing two $GdTiO_3/SrTiO_3$ interfaces. If each repeat contributes the same sheet carrier density as the $x = 1$ trilayer, then the sheet

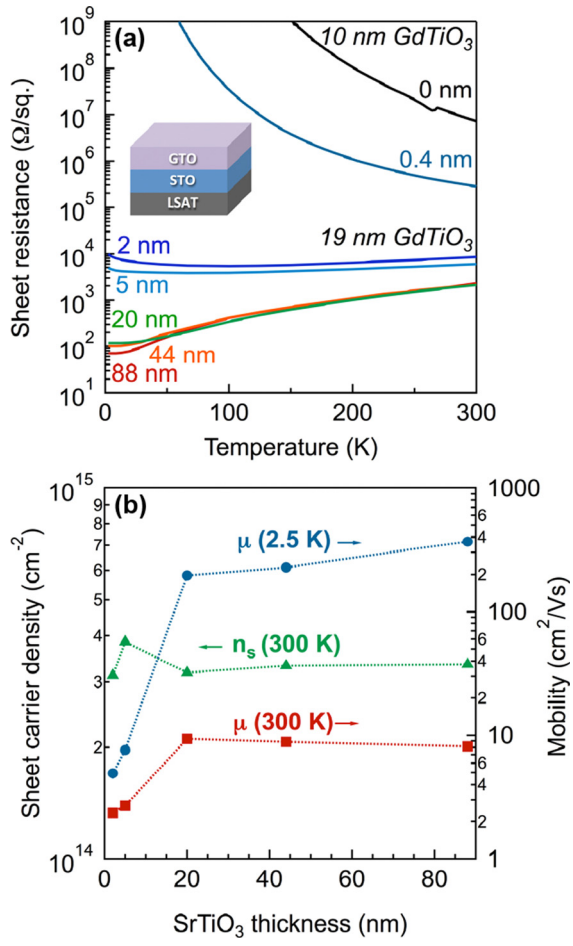

FIG. 1. (Color online) (a) Sheet resistance as a function of temperature for $GdTiO_3/SrTiO_3$/LSAT structures with varying $SrTiO_3$ thicknesses, indicated by the labels. The $GdTiO_3$ film grown directly on LSAT is labeled "0 nm." (b) Sheet carrier density and mobility at room temperature and 2.5 K.

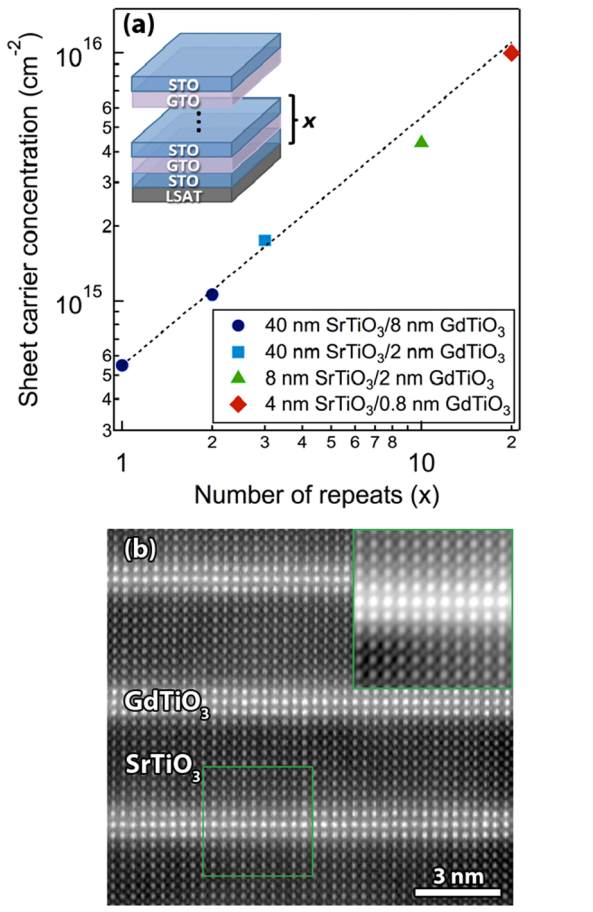

FIG. 2. (Color online) (a) Room temperature sheet carrier concentrations of $SrTiO_3/GdTiO_3/SrTiO_3$ multilayers as a function of multilayer repeats (x). The dashed line indicates the expected sheet carrier concentration scaling with number of repeats as calculated from the $x = 1$ sample. (b) High-angle annular dark-field scanning transmission electron microscopy image of the $x = 20$ multilayer.

density should scale as shown by the dashed line. The experimental results closely follow the dashed line, independent of $GdTiO_3$ or $SrTiO_3$ thicknesses. The total carrier sheet density is not proportional to the total Gd in the superlattice nor is it proportional to the Gd concentration. It is proportional to the number of interfaces. The constant sheet carrier density per interface excludes interfacial intermixing as the source of the charge carriers, because the charge carrier density in this case should strongly dependent on the precise interfacial composition.[20] Figure 2(b) shows a high-angle annular dark-field scanning transmission electron microscopy (HAADF/STEM) image of the sample with $x = 20$. Thicker sample regions appear to show intermixing of about one monolayer, but observation of thinner regions[29] shows that the interface contains short steps, which overlap along the beam direction. Thus the interfaces are *locally* atomically abrupt. Comparison of sheet carrier densities of the $x = 1$ multilayer (two $GdTiO_3/SrTiO_3$ interfaces) with that of the $GdTiO_3/SrTiO_3$/LSAT structures (one interface) of Fig. 1(b) shows that the sheet carrier concentration of the multilayer is slightly less than twice that of a single interface. This is likely due to different electrostatic boundary conditions for $GdTiO_3/SrTiO_3$ and $SrTiO_3/GdTiO_3$ interfaces.

The interfacial space charge can be understood by noting that the fixed polar charge at the interface must be neutralized by negative space charge, mobile or fixed, and dictated by the available quantum states in the presence of the selfconsistent electrostatic fields/potentials. The $SrTiO_3$ is *n*-type (oxygen deficient) and $GdTiO_3$ is *p*-type. The fixed polar charge can be neutralized by an accumulation layer in the $SrTiO_3$, a hole depletion layer (negatively charged acceptors) in the $GdTiO_3$ and an inversion layer in the $GdTiO_3$. The mobile charge is close to that required to compensate the fixed polar charge at the interface: thus hole depletion in the $GdTiO_3$ is not sufficient to siphon off significant numbers of electrons from the mobile space charge. The interface may share the mobile charge between the $SrTiO_3$ and the $GdTiO_3$. The relatively strong temperature dependence of the electron mobility [Fig. 1(b)] and the absence of an anomalous Hall effect, potentially caused by the ferrimagnetism in the $GdTiO_3$, indicate that mobile charge is largely found on the $SrTiO_3$ side and that the conduction band alignment favors $SrTiO_3$ accumulation. Because $SrTiO_3$ has the larger band gap, the band line-up must be of type II (staggered). First principle calculations confirm this.[29] The mobile charge distribution and band bending are modeled using a self consistent Poisson-Schrödinger solver,[30] as shown in Fig. 3, using band lineups from first-principle calculations,[29] a fixed interface charge of $3.4 \times 10^{14}\,cm^{-2}$ (modeled as a 0.2 nm layer with fully ionized dopants), an electron effective mass of 1 m_0, a 6-fold degeneracy of the conduction band, and dielectric constants of $SrTiO_3$ and $GdTiO_3$ of 300 and 30, respectively. The interfacial positive charge induces a high-density 2DEG. A deep quantum well is formed [Fig. 3(b)], but there is overflow of the electrons into the $GdTiO_3$. Despite the high effective mass/density of states, the high electron density drives the Fermi level above the $SrTiO_3$ conduction band minimum by approximately 0.7 eV, which is greater than the assumed conduction band offset. The $GdTiO_3$ conduction band is therefore near

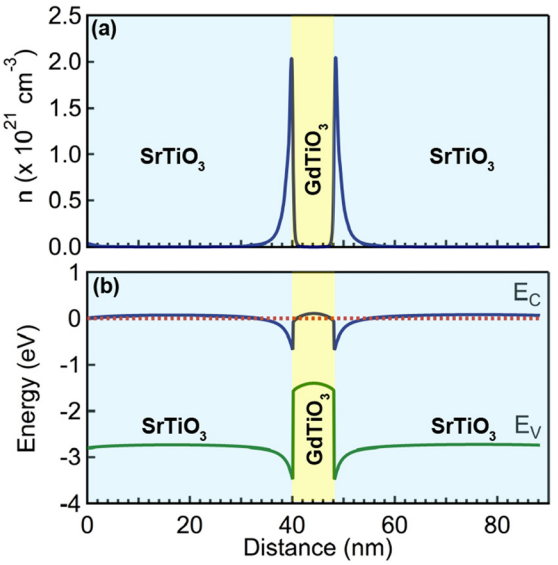

FIG. 3. (Color online) Calculated (a) charge distribution and (b) band alignment for a $SrTiO_3/GdTiO_3/SrTiO_3$ heterostructure. The Fermi level is shown as a dotted line.

the Fermi level near the interface and the polar charges inverts the *p*-type $GdTiO_3$ ($N_A = 3 \times 10^{19}\,cm^{-3}$), making it effectively *n*-type. From the simulations, the spatial extent of the quantum confined electron gas is ~3 nm. We note that the superlattice with only 4 nm $SrTiO_3$ is best described as a quantum well rather than two distinct interface space charge layers, yet the total electron density appears fixed by the polarization charge.

The model supports experimental observations, namely, that the mobile space charge density at the $GdTiO_3/SrTiO_3$ interface is perturbed very little by the LSAT even for small separations and that the transport is dominated by one carrier type. The electrical transport measurements indicate that the different 2DEG regions in multi-layer structures are not isolated, which may have been expected since the $GdTiO_3$ layers are *p*-type. Most importantly, the very tight binding of the electrons to the interface should allow for exploration of quantum and strong correlation effects. Figure 3 is based on an effective mass model that assumes slowly varying envelope wave functions. The wavefunctions are derived from *d*-bands that are likely better described by tight binding Hamiltonians with rapid spatial variations, far from the approximations used in conventional semiconductor heterostructures. Appropriate models need to be developed, especially those that also include electron correlations.

P.M. and J.Y.Z. were supported through awards from the U.S. National Science Foundation (Grant No. DMR-1006640) and DOE Basic Energy Sciences (Grant No. DEFG02-02ER45994). T.A.C. was supported through the Center for Energy Efficient Materials, an Energy Frontier Research Center funded by the DOE (Award Number DE-SC0001009). S.S., S.J.A., and D.G.O. acknowledge support through a MURI program of the Army Research Office (Grant No. W911-NF-09-1-0398). The work made use of the UCSB Nanofabrication Facility, a part of the NSF-funded NNIN network.

[1]A. Ohtomo, D. A. Muller, J. L. Grazul, and H. Y. Hwang, Nature **419**, 378 (2002).
[2]S. Okamoto and A. J. Millis, Nature **428**, 630 (2004).
[3]C. Yoshida, H. Tamura, A. Yoshida, Y. Kataoka, N. Fujimaki, and N. Yokoyama, Jpn. J. Appl. Phys. Part 1 **35**, 5691 (1996).
[4]S. Smadici, P. Abbamonte, A. Bhattacharya, X. Zhai, B. Jiang, A. Rusydi, J. N. Eckstein, S. D. Bader, and J.-M. Zuo, Phys. Rev. Lett. **99**, 196404 (2007).
[5]J. Garcia-Barriocanal, F. Y. Bruno, A. Rivera-Calzada, Z. Sefrioui, N. M. Nemes, M. Garcia-Hernandez, J. Rubio-Zuazo, G. R. Castro, M. Varela, S. J. Pennycook, Carlos Leon, and J. Santamaria, Adv. Mater. **22**, 627 (2010).
[6]J. Garcia-Barriocanal, J. C. Cezar, F. Y. Bruno, P. Thakur, N. B. Brookes, C. Utfeld, A. Rivera-Calzada, S. R. Giblin, J. W. Taylor, J. A. Duffy, S. B. Dugdale, T. Nakamura, K. Kodama, C. Leon, S. Okamoto, and J. Santamaria, Nat. Commun. **1**, 82 (2010).
[7]Z. S. Popovic and S. Satpathy, Phys. Rev. Lett. **94**, 176805 (2005).
[8]Pseudocubic notation is used here for the orthorhombic $RTiO_3$.
[9]G. A. Baraff, J. A. Appelbaum, and D. R. Hamann, Phys. Rev. Lett. **38**, 237 (1977).
[10]W. A. Harrison, E. A. Kraut, J. R. Waldrop, and R. W. Grant, Phys. Rev. B **18**, 4402 (1978).
[11]S. A. Chambers, Surf. Sci. **605**, 1133 (2011).
[12]D. G. Schlom and J. Mannhart, Nat. Mater. **10**, 168 (2011).
[13]D. O. Klenov, D. G. Schlom, H. Li, and S. Stemmer, Jpn. J. Appl. Phys. Part 2 **44**, L617 (2005).
[14]J. Mannhart, D. H. A. Blank, H. Y. Hwang, A. J. Millis, and J. M. Triscone, MRS Bull. **33**, 1027 (2008).
[15]R. Ohtsuka, M. Matvejeff, K. Nishio, R. Takahashi, and M. Lippmaa, Appl. Phys. Lett. **96**, 192111 (2010).
[16]J. S. Kim, S. S. A. Seo, M. F. Chisholm, R. K. Kremer, H. U. Habermeier, B. Keimer, and H. N. Lee, Phys. Rev. B **82**, 201407 (2010).
[17]M. Huijben, A. Brinkman, G. Koster, G. Rijnders, H. Hilgenkamp, and D. H. A. Blank, Adv. Mater. **21**, 1665 (2009).
[18]A. D. Caviglia, S. Gariglio, N. Reyren, D. Jaccard, T. Schneider, M. Gabay, S. Thiel, G. Hammerl, J. Mannhart, and J. M. Triscone, Nature **456**, 624 (2008).
[19]S. Thiel, G. Hammerl, A. Schmehl, C. W. Schneider, and J. Mannhart, Science **313**, 1942 (2006).
[20]Y. Tokura, Y. Taguchi, Y. Okada, Y. Fujishima, T. Arima, K. Kumagai, and Y. Iye, Phys. Rev. Lett. **70**, 2126 (1993).
[21]S. S. A. Seo, W. S. Choi, H. N. Lee, L. Yu, K. W. Kim, C. Bernhard, and T. W. Noh, Phys. Rev. Lett. **99**, 266801 (2007).
[22]A. Schmehl, F. Lichtenberg, H. Bielefeldt, J. Mannhart, and D. G. Schlom, Appl. Phys. Lett. **82**, 3077 (2003).
[23]H. D. Zhou and J. B. Goodenough, J. Phys.: Condens. Matter **17**, 7395 (2005).
[24]D. A. Crandles, T. Timusk, J. D. Garrett, and J. E. Greedan, Physica C **201**, 407 (1992).
[25]A. Ohtomo, D. A. Muller, J. L. Grazul, and H. Y. Hwang, Appl. Phys. Lett. **80**, 3922 (2002).
[26]K. S. Takahashi, M. Onoda, M. Kawasaki, N. Nagaosa, and Y. Tokura, Phys. Rev. Lett. **103**, 057204 (2009).
[27]B. Jalan, R. Engel-Herbert, N. J. Wright, and S. Stemmer, J. Vac. Sci. Technol. A **27**, 461 (2009).
[28]P. Moetakef, J. Y. Zhang, A. Kozhanov, B. Jalan, R. Seshadri, S. J. Allen, and S. Stemmer, Appl. Phys. Lett. **98**, 112110 (2011).
[29]See supplemental material at http://dx.doi.org/10.1063/1.3669402 for structural data, Hall resistance as a function of magnetic field and details of the first principle calculations of the $GdTiO_3/SrTiO_3$ band offsets.
[30]M. Grundmann, BandEng program (unpublished).